Monolayers of Hexadecyltrimethylammonium *p*-Tosylate at the Air−Water Interface. 1. Sum-Frequency Spectroscopy

G. R. Bell, Z. X. Li, and C. D. Bain*

Physical and Theoretical Chemistry Laboratory, University of Oxford, South Parks Road, Oxford, OX1 3QZ, United Kingdom

P. Fischer and D. C. Duffy

Department of Chemistry, University of Cambridge, Lensfield Road, Cambridge, CB2 1EW, United Kingdom

Received: May 6, 1998; In Final Form: July 28, 1998

Sum-frequency vibrational spectroscopy has been used to determine the structure of monolayers of the cationic surfactant, hexadecyltrimethylammonium *p*-tosylate ($C_{16}TA^+Ts^-$), at the surface of water. Selective deuteration of the cation or the anion allowed the separate detection of sum-frequency spectra of the surfactant and of counterions that are bound to the monolayer. The *p*-tosylate ions are oriented with their methyl groups pointing away from the aqueous subphase and with the C_2 axis tilted, on average, by 30−40° from the surface normal. The vibrational spectra of $C_{16}TA^+$ indicate that the number of gauche defects in the monolayer does not change dramatically when bromide counterions are replaced by *p*-tosylate. The ends of the hydrocarbon chains of $C_{16}TA^+$ are, however, tilted much further from the surface normal in the presence of *p*-tosylate than in the presence of bromide. A quantitative analysis of the sum-frequency spectra requires a knowledge of the molecular hyperpolarizability tensor: the role of ab initio calculations and Raman spectroscopy in determining the components of this tensor is discussed.

1. Introduction

When charged surfactants form micelles, charge neutrality requires that an equal number of oppositely charged ions are associated with the micelle.[1] These counterions can reside benignly in the diffuse part of the electrical double layer or can interact specifically with the surfactant molecules. These specific interactions have a profound effect on the geometry of the aggregate and on physical properties of surfactant solutions. Much experimental and theoretical work has been carried out to understand these effects,[2−4] but the interactions that control them are still poorly understood. The intermolecular forces that exist between counterions and micelles in solution also operate in monolayers of surfactants at the air−water interface. Monolayers can provide structural information that is difficult to obtain from micelles. The surface of water provides a reference plane and the surface normal a reference direction from which the location and orientation of the surfactant and counterion can be measured. Randomly oriented micelles present no such convenient references, and shear forces or magnetic anisotropy has to be exploited to induce some degree of orientation into the aggregates. The study of monolayers does, however, require specialized surface-sensitive techniques. Here we present the results of two such techniques, sum-frequency spectroscopy (SFS) and neutron reflection (NR), applied to a monolayer of a cationic surfactant, hexadecyltrimethylammonium *p*-tosylate ($C_{16}TA^+Ts^-$), adsorbed at the air−water interface. In the first of two papers, we present vibrational spectra of the monolayer obtained by infrared−visible sum-frequency generation and discuss the interpretation of the spectra in terms of the structure of the monolayer. In the accompanying paper, we present results obtained by neutron reflection and discuss the relevance of the structure of the monolayer to aggregation in bulk solution.[5]

A preliminary communication summarizing the main structural features of the monolayer has been published previously.[6] The larger part of these two papers is devoted to a detailed analysis of the experimental data. To help readers follow the arguments, we provide a brief summary of the final conclusions here. The addition of *p*-tosylate to a solution of $C_{16}TAB$ increases the area per surfactant molecule by 25%, in contrast to the normal affect of salt, which is to decrease the area per molecule. Eighty percent of the tosylate counterions are bound to the monolayer; the remaining 20% are presumed to lie in the diffuse double layer. The tosylate ions lie deep within the hydrophobic region of the monolayer: the center of the distribution of the tosylate ions is coplanar with the sixth methylene unit of the hydrocarbon chain, counting from the polar end. The counterions are tilted, on average, 30−40° from the surface normal with the hydrophobic part of the ions oriented away from the water. Addition of *p*-tosylate results in an increase in the tilt of the outermost part of the hydrocarbon chain of the surfactant, consistent with the maintenance of a liquidlike density in the monolayer. In bulk solutions, addition of *p*-tosylate causes a sphere-to-rod transition in the micellar geometry. In the following paper, we show how the structure of the monolayer can be used to rationalize this transition within a simple geometric model of micellar aggregation.

SFS is a form of nonlinear optical spectroscopy that provides vibrational spectra of molecules in noncentrosymmetric environments.[7] SFS is only sensitive to molecules at interfaces where the centrosymmetry of isotropic bulk phases is broken. Sum-frequency (SF) spectra not only provide a characteristic

* Corresponding author. E-mail Colin.Bain@chem.ox.ac.uk.

10.1021/jp982142+ CCC: $15.00
Published on Web 10/30/1998

"fingerprint" of the molecules at the surface but also contain intrinsic information on the surface structure. Analysis of SF spectra yields the polar orientation and tilt of molecules adsorbed at surfaces.[7] Interpretation of the C−H stretching modes in the SF spectra of long hydrocarbon chains has been especially fruitful in determining the conformational order in surfactant monolayers.[8,9]

Both aromatic counterions and surfactant monolayers have vibrational modes that are SF-active. We have previously used SFS to study the binding of counterions to surfactant monolayers at the solid−water interface.[10−13] Initial experiments were performed on the pseudohalides, thiocyanate (SCN^-)[10] and cyanide (CN^-),[12,13] coadsorbed with the tetradecyltrimethylammonium ion ($C_{14}TA^+$) at a hydrophobic surface. The C−N stretching modes in the SF spectra showed that both the SCN^- and CN^- ions were bound to the monolayer with the nitrogen atom furthest from the solid substrate. This study was extended to three aromatic counterions: *p*-tosylate, benzoate, and salicylate.[11] All three counterions were bound to the monolayer with their aromatic rings oriented away from the aqueous phase. In the one previous study of counterion binding to surfactant monolayers at the air−water interface, we showed that benzoate ions bound to a monolayer of $C_{14}TA^+$ were oriented close to the surface normal.[14]

In neutron reflection, the reflectivity of a neutron beam is measured as a function of momentum transfer perpendicular to the surface of water.[15] Reflectivity curves depend on the scattering amplitudes and densities of the molecules at the surface and can be analyzed to yield the area per molecule and the thickness of the film.[16] NR has been applied extensively in the study of surfactants adsorbed at the air−water interface.[15−17] Since hydrogen and deuterium atoms scatter neutrons out of phase with each other, a mixture of H_2O and D_2O can be produced in which the scattering from the hydrogen atoms exactly cancels the scattering from O and D. Neutrons are not reflected from the interface between air and such a mixture: this mixture is referred to as null-reflecting water (nrw). Deuterated surfactants scatter neutrons strongly and can be detected readily at the surface of nrw. Since coherent scattering from protonated surfactants is weak, selective deuteration of the surfactant and its counterion allows the surface coverage of each to be measured independently. More complex experiments involving partial deuteration yield the relative locations of the counterion and surfactant molecules.[5]

The salts of $C_{16}TA^+$ have a rich solution chemistry that has been the subject of extensive studies. $C_{16}TA^+$ is a single-chain cationic surfactant that forms small (∼50 Å diameter) spherical micelles above the critical micellar concentration (cmc) in the presence of simple inorganic ions such as bromide. At high concentrations, or in the presence of large amounts of salt ([NaBr] > 0.1 M), elongated, rod-shaped micelles are observed.[18] The sphere-to-rod transition at high ionic strength is ascribed to a reduction in repulsions between the cationic headgroups due to electrostatic screening by counterions. This transition is observed with most (but not all) inorganic ions: counterions that interact very weakly with the surfactant (e.g., Cl^-) are ineffective in screening the repulsions between the headgroups. Some aromatic anions can induce a sphere-to-rod transition at much lower concentrations (∼1 mM). The first example, the salicylate ion, was discovered more than 20 years ago[2] and has been studied extensively since.[3] Many other cationic surfactant−counterion combinations have been identified that form rod-shaped aggregates at low concentrations,[4] including the system we study here: $C_{16}TAB$ + *p*-tosylate.[19]

The transition from small spherical micelles to aggregates with rodlike structures can have a remarkable effect on the rheological and optical properties of the surfactant solution.[2−4,19,20] For example, a solution of $C_{16}TAB$ at its cmc has a low viscosity and is optically isotropic. In the presence of 2 mM sodium salicylate, the solution becomes highly viscous, and trapped air bubbles are seen to recoil, indicating that the solution has elastic properties. The solution is also optically birefringent under shear.[3] Cylindrical micelles exist in solutions of $C_{16}TAB$ + *p*-tosylate at an anion concentration of 1 mM, and viscoelastic properties are observed at higher concentrations (20 mM). The solutions also display flow birefringence.[19] These unusual properties arise from interactions between elongated micelles.[4] For example, viscoelasticity occurs when the micelles reach a critical length, become entangled, and can no longer flow easily past one another; flow birefringence and iridescence arise from alignment of the micelles.[4] These surfactant systems show many similarities to polymer solutions in the semidilute regime.[21] One of the intriguing features of these properties is the sensitivity to subtle differences in the molecular structure of counterions. For example, solutions of $C_{16}TAB$ become viscoelastic if *p*-dichlorobenzoate is added, while *o*-dichlorobenzoate has no effect.[2] Conversely, *o*-hydroxybenzoate (salicylate) causes viscoelasticity but *p*-hydroxybenzoate does not.[2,22]

Several techniques provide information on the molecular structure of these surfactant aggregates. Light scattering[23] and small-angle neutron scattering (SANS)[24] yield the size, geometry, and number of surfactant molecules in the aggregate. Cryo-transmission electron microscopy provides direct images of entangled rodlike structures.[4a,25] Low-angle X-ray diffraction (XRD) has been used to study the long-range order of these aggregates in solution.[26] ^1H and ^{13}C NMR are particularly informative:[27−31] the polarity of the environment alters the ^{13}C chemical shifts in the aromatic anions, and the ring current of the benzene ring changes the chemical shift of protons in the hydrocarbon chains of the surfactant that are near the ring. The ^{13}C chemical shifts indicate that the benzene rings of many aromatic anions reside in a region less polar than water, presumably within the micelle. From the relative chemical shifts of the ortho, meta, and para protons, some workers have attempted to determine the average orientation of the counterions.[27−29] The $C_{16}TAB$ + *p*-tosylate system we study here has been characterized previously in the bulk phase by fluorescence,[32] FTIR, XRD, microscopy, and NMR.[19]

NMR studies have stimulated debate on the relationship between the ability of a counterion to induce sphere-to-rod transitions and the orientation and position of the counterion within the aggregate. Iyer et al.[28] asserted that viscoelasticity was correlated with the orientation of the counterions. Their observations indicated that hydroxybenzoate counterions with their COO^- group oriented perpendicular to the micellar surface induced viscoelasticity, whereas counterions with the COO^- group oriented parallel to the surface did not. Bachofer demurred and provided the counterexample of *o*-toluate anions, which do not induce viscoelastic behavior but have their COO^- groups oriented perpendicular to the surface.[29a] Bachofer preferred a geometric model proposed by Israelachvili et al.,[33] in which the structure of a surfactant aggregate is determined by V/al, where V is the volume of the hydrocarbon tail, a is the effective area of the charged headgroup, and l is the maximum effective length of the hydrocarbon chain. For values of $V/al < 1/3$, the formation of structures with high curvature, such as spheres, is favored; higher values of V/al result in the formation of structures with lower curvature such as rods and sheets. The

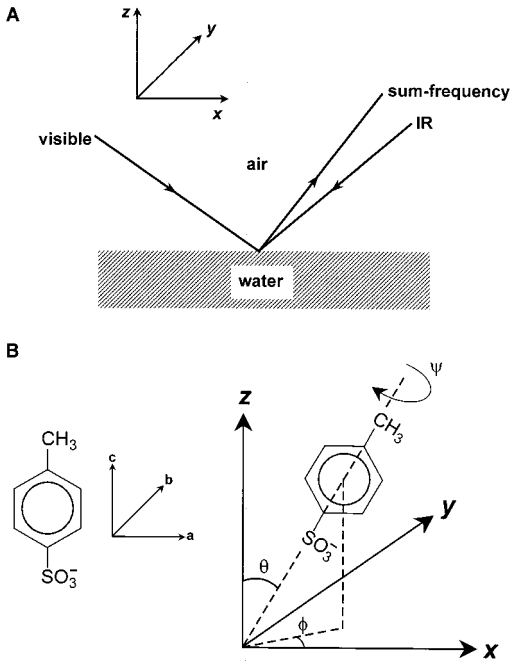

Figure 1. (A) Geometry of the SF experiment. The Cartesian axes of the surface are shown. (B) Definition of Euler angles used in text.

influence of counterions is then rationalized in terms of changes in V and a. Magid reached a similar conclusion from an NMR study of dichlorobenzoates bound to C_{16}TAB micelles.[27] She found that aromatic anions that induced viscoelasticity penetrated more deeply into the micellar core than anions that did not. Smith et al.[22] suggested that only those ions in which both the hydrophobic and hydrophilic groups can reside in their preferred environments promote sphere-to-rod transitions. Despite this large number of studies, the molecular interactions that control sphere-to-rod transitions are not fully understood.

2. Sum-Frequency Spectroscopy (SFS)

In SFS, two pulsed laser beams, one in the visible (ω_{vis}) and the other in mid-IR (ω_{IR}), are overlapped at a surface, and the light emitted at the sum-frequency ($\omega_{sum} = \omega_{vis} + \omega_{IR}$) is detected.[7] The signal detected at the sum-frequency (S_{sum}) depends on the second-order nonlinear susceptibility of the surface, $\chi^{(2)}_{ijk}$, and the intensities of the incident laser beams, I_{vis} and I_{IR}. Within the electric dipole approximation, the signal (in photons per pulse) is given by[34]

$$S_{sum} = \frac{2\epsilon_0 A\tau \cos\theta_{sum} I_{vis} I_{IR}}{\hbar\omega_{sum} c}\left|\sum_{ijk} L_i(\omega_{sum})\chi^{(2)}_{ijk} K_j(\omega_{vis}) K_k(\omega_{IR})\right|^2, \quad ijk = xyz \quad (1)$$

$K_j(\omega_{vis})$ and $K_k(\omega_{IR})$ are the ratio of the electric fields at the surface to the electric fields in air; $L_i(\omega_{sum})$ relates the polarization at the sum-frequency (SF) to the electric field of the emitted SF light in the bulk medium (in this case, air); A and τ are the spatial and temporal overlap of the laser beams at the surface; θ_{sum} is the angle between the wavevector of the emitted SF light and the surface normal, and xyz refer to the Cartesian surface-fixed axes. The experimental geometry is shown in Figure 1A.

The susceptibility can be broken down into two parts: a resonant term, $\chi^{(2)}_{ijk,R}$, arising from the vibrational modes of adsorbed molecules and a nonresonant term, $\chi^{(2)}_{NR}$, arising from the nonlinear response of the substrate. $\chi^{(2)}_{ijk,R}$ is a macroscopic property of the interface and is related to the microscopic hyperpolarizability, β_{lmn}, of the individual molecules in the interface averaged over all their orientations:

$$\chi^{(2)}_{ijk,R} = f\frac{N}{\epsilon_0}\langle\beta_{lmn}\rangle, \quad lmn = abc \quad (2)$$

N is the number of the molecules per unit area, f relates the local electric field experienced by the molecules to the macroscopic electric field in the medium, and abc refer to the Cartesian molecular axes. $\chi^{(2)}$ and β are third-rank tensors that change sign under inversion. In the bulk phase, the surfactant molecules are randomly oriented, and therefore the orientational average over β will vanish: the contribution from molecules with one orientation will be canceled by an equal number of molecules with the opposite orientation. The interface breaks the symmetry of the bulk phases. The different forces acting on the two sides of the interface generally result in a preferred orientation of molecules at the surface. The monolayers we consider here are azimuthally isotropic but are asymmetric in the direction normal to the surface. This asymmetry leads to nonzero values of $\chi^{(2)}$ and hence to the emission of sum-frequency light.[35]

When the frequency of the IR laser is close to a molecular vibrational frequency, β_{lmn} can be expressed in terms of the IR and Raman transition dipole moments, μ'_n and α'_{lm}[36]

$$\beta_{lmn} = \frac{\alpha'_{lm}\mu'_n}{2\hbar(\omega_v - \omega_{IR} - i\Gamma_v)} \quad (3)$$

ω_v is the frequency of a vibrational mode, and Γ_v is its homogeneous line width. When the IR laser is in resonance with an IR- and Raman-active vibrational mode of the molecules at the surface, $\chi^{(2)}_{ijk,R}$ increases. By scanning the frequency of the IR laser and detecting the intensity of the SF light, we can therefore obtain a vibrational spectrum of the adsorbed molecules.

Interpretation of sum-frequency vibrational spectra is complicated by the fact that $\chi^{(2)}$ generally contains contributions from several modes, ν, in addition to the nonresonant background from the substrate:

$$\chi^{(2)} = \chi^{(2)}_{NR} + \sum_\nu \chi^{(2)}_{ijk,R} \quad (4)$$

Since the SF signal depends on $|\chi^{(2)}|^2$, these contributions are convoluted with one another, and the resulting line shapes depend strongly on the relative phases and strengths of $\chi^{(2)}_{ijk,R}$ and $\chi^{(2)}_{NR}$.

The K and L terms in eq 1 can be collated into overall Fresnel factors, $F_{ijk} = L_i(\omega_{sum}) K_j(\omega_{vis}) K_k(\omega_{IR})$. The SF signal can then be written as

$$S_{sum} = k'\left|\sum_{ijk} F_{ijk}\chi^{(2)}_{ijk}\right|^2 \quad (5)$$

where k' is a constant that depends on the lasers and the experimental geometry. For monolayers that are isotropic in the plane of the surface, there are only four independent components of $\chi^{(2)}_{ijk}$: $\chi^{(2)}_{zzz}$, $\chi^{(2)}_{xxz} = \chi^{(2)}_{yyz}$, $\chi^{(2)}_{xzx} = \chi^{(2)}_{yzy}$, $\chi^{(2)}_{zxx} = \chi^{(2)}_{zyy}$. If the frequencies of the SF and visible beams are far removed from electronic resonances in the molecules, then the Raman tensor is symmetric and $\chi^{(2)}_{xzx} = \chi^{(2)}_{zxx}$.[37]

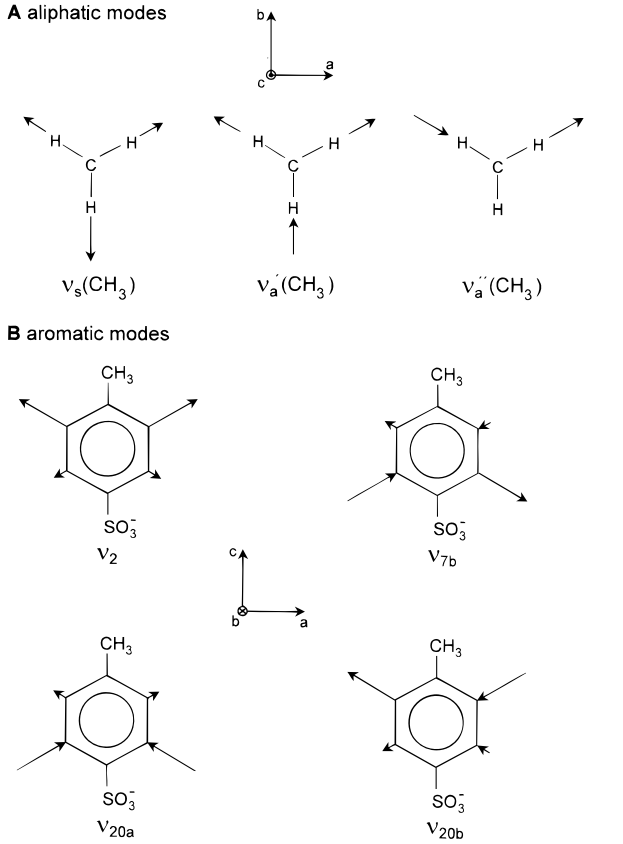

Figure 2. Normal modes of *p*-tosylate observed in SF spectra. The labeling of the aromatic modes follows that of Wilson (ref 39). The lengths of the C−H bonds shown are proportional to the bond displacements of the modes calculated ab initio. The Cartesian axes of the *p*-tosylate molecule are shown.

Different components of $\chi^{(2)}_{ijk}$ can be probed with different polarizations of the electric fields at the interface. For monolayers that are azimuthally isotropic, only four combinations of polarization give rise to SF emission: ssp, sps, pss, and ppp, where the letters designate the polarizations of the SF, visible, and IR beams, respectively. The first three polarization combinations depend on a single component of $\chi^{(2)}$, while the fourth combination contains an admixture of all four independent components:

$$S_{ssp} = k'|F_{yyz}\chi_{yyz}|^2 \tag{6a}$$

$$S_{sps} = k'|F_{yzy}\chi_{yzy}|^2 \tag{6b}$$

$$S_{pss} = k'|F_{zyy}\chi_{zyy}|^2 \tag{6c}$$

$$S_{ppp} = k'|F_{zxx}\chi_{zxx} + F_{xzx}\chi_{xzx} + F_{xxz}\chi_{xxz} + F_{zzz}\chi_{zzz}|^2 \tag{6d}$$

If $\chi_{yzy} = \chi_{zyy}$, sps- and pss-polarized spectra differ only in intensity through differences in the Fresnel coefficients.

The susceptibilities are related to the molecular hyperpolarizability by a sixth-rank matrix of direction cosines, which have been tabulated by Hirose.[38] The components of the transformation matrix depend on the Euler angles (θ,ψ,ϕ) relating the molecular and laboratory axis systems (Figure 1B). In this paper, we will be concerned with the interpretation of the CH_3 symmetric stretching mode of the surfactant and the aliphatic and aromatic C−H stretching modes of the *p*-tosylate ion. The molecular axis systems are shown in Figure 2. The azimuthal angle, ϕ, between the projection of the *c*-axis in the *xy*-plane and the *x*-axis is randomly distributed since the surface is isotropic in the plane. We further assume that the distribution of angles ψ is isotropic, where ψ is the angle between the *a*-axis and the *cz*-plane; i.e., we assume that the twists of the molecules about the *c*-axis are random. The components of the transformation matrix can therefore be averaged over ϕ and ψ and are then solely a function of the tilt angle, θ, between the *c*-axis and the surface normal. It is this angle, θ, that we seek to determine from a quantitative analysis of the SF spectra.

The modes we observe in *p*-tosylate have either A_1 or B_1 symmetry in the C_{2v} point group that results from free rotation of the CH_3 and SO_3^- groups. For the A_1 modes, there are three nonzero components of the hyperpolarizability: β_{aac}, β_{bbc}, and β_{ccc}. Expressions that relate $\chi^{(2)}$ to β for the symmetric methyl modes are given elsewhere;[9] for the C−H stretching modes of the ring, we can ignore β_{bbc}, and the resulting expressions for $\chi^{(2)}$ are

$$\chi^{(2)}_{zzz} = \frac{Nf}{8\epsilon_0}(\langle\cos\theta\rangle(6t+1) - \langle\cos 3\theta\rangle(1-2t))\beta_{aac} \tag{7a}$$

$$\chi^{(2)}_{xxz} = \frac{Nf}{16\epsilon_0}(\langle\cos\theta\rangle(2t+7) + \langle\cos 3\theta\rangle(1-2t))\beta_{aac} \tag{7b}$$

$$\chi^{(2)}_{xzx} = \frac{Nf}{16\epsilon_0}(\langle\cos\theta\rangle(2t-1) - \langle\cos 3\theta\rangle(1-2t))\beta_{aac} \tag{7c}$$

where $t = \beta_{ccc}/\beta_{aac}$. For the B_1 modes,

$$\chi^{(2)}_{zzz} = \frac{Nf}{4\epsilon_0}(\langle\cos\theta\rangle - \langle\cos 3\theta\rangle)\beta_{aca} \tag{7d}$$

$$\chi^{(2)}_{xxz} = \frac{Nf}{8\epsilon_0}(\langle\cos\theta\rangle - \langle\cos 3\theta\rangle)\beta_{aca} \tag{7e}$$

$$\chi^{(2)}_{xzx} = \frac{Nf}{8\epsilon_0}(3\langle\cos\theta\rangle + \langle\cos 3\theta\rangle)\beta_{aca} \tag{7f}$$

To determine θ from experimental data, we generally need to know the components of the hyperpolarizability tensor which, in turn, implies a knowledge of the infrared and Raman transition dipole moments (eq 3). It is easier to work with ratios of susceptibilities, since then only the relative values of different components of β are required. The relative magnitudes of the components of the IR transition dipole moment can usually be estimated by symmetry or from IR spectra. The Raman tensor provides a greater challenge. Rarely are the individual components of the Raman tensor known experimentally. For some molecules a Raman depolarization ratio has been measured, but this ratio is only useful in the context of a Raman tensor with only two independent components, and even then ambiguities remain. Hyperpolarizabilities can also be calculated ab initio, but the computer time required to obtain quantitative results for large molecules remains prohibitive. The extent to which these problems can be resolved for different modes in *p*-tosylate is discussed in section 4.

3. Experimental Section

The laser system in Oxford has been described in detail elsewhere.[9] The IR laser beam (2800−3100 cm^{-1}, 20 Hz, ~1 ns, 1 mJ/pulse, <0.2 cm^{-1} bandwidth, <1 mm diameter) and visible beam (532 nm, 3.5 ns, 10 mJ/pulse, 2 mm diameter) were overlapped at the surface of water. The IR and visible beams were incident at the surface at angles of 50° and 55°,

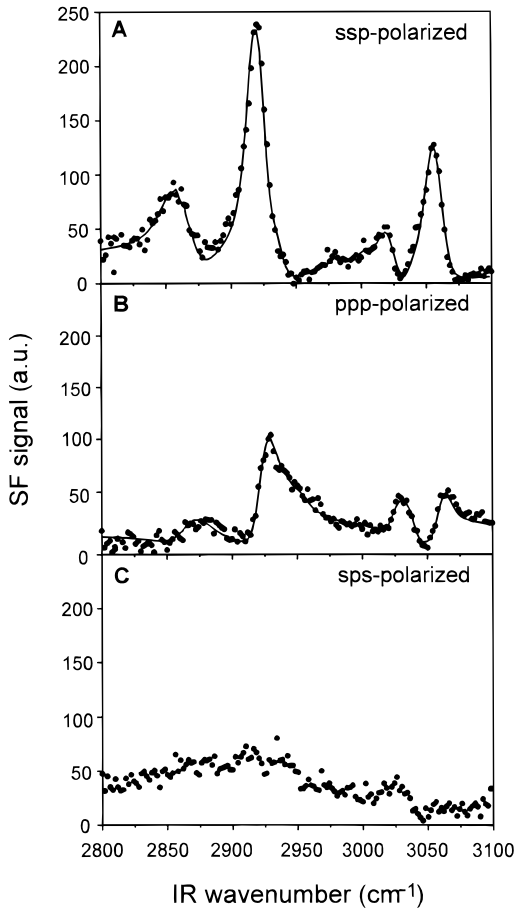

Figure 3. SF spectra in the C−H stretching region of surfaces of solutions containing 1 mM $dC_{16}TAB$ and 3 mM sodium *p*-tosylate (Na hTs) in D_2O. The spectra were acquired with (A) ssp-, (B) ppp-, and (C) sps-polarized laser beams. The solid lines are computer fits to the spectra (see text).

respectively, in a counterpropagating geometry (Figure 1). These angles of incidence are a compromise between the angles that optimize the Fresnel coefficients for the different polarization combinations. The counterpropagating geometry is chosen for experimental convenience. A copropagating geometry would not change ssp- and sps-polarized spectra but would alter the appearance of ppp-polarized spectra since F_{zxx} and F_{xzx} in eq 6d would change sign. The emitted SF light was filtered to remove scattered visible light and detected by a liquid nitrogen cooled CCD (Princeton Instruments). Small fractions of the IR and visible beams were split off and focused onto a GaAs crystal to generate a reference SF signal, which was detected simultaneously on the CCD. After both SF signals were corrected for background, the sample signal was divided by the reference signal to provide normalization for the variation in the IR and visible pulse energies.

SF spectra were acquired from the surfaces of solutions of D_2O containing 1 mM $C_{16}TAB$ and 3 mM sodium *p*-tosylate. The solutions were contained in a 50 mm diameter glass sample dish, which was rotated at 14 rpm to reduce heating of the surface by the laser beams. The temperature of the dish was kept constant at 298 K. Glassware was cleaned in alkaline detergent (Decon 90) and checked for cleanliness by ellipsometry.

SF spectra of the *p*-tosylate ion in the C−H stretching region (Figure 3) were acquired from solutions containing chain-deuterated surfactant ($dC_{16}TAB$) and perprotonated *p*-tosylate (hTs). Spectra with ssp-, ppp-, and sps-polarized beams were

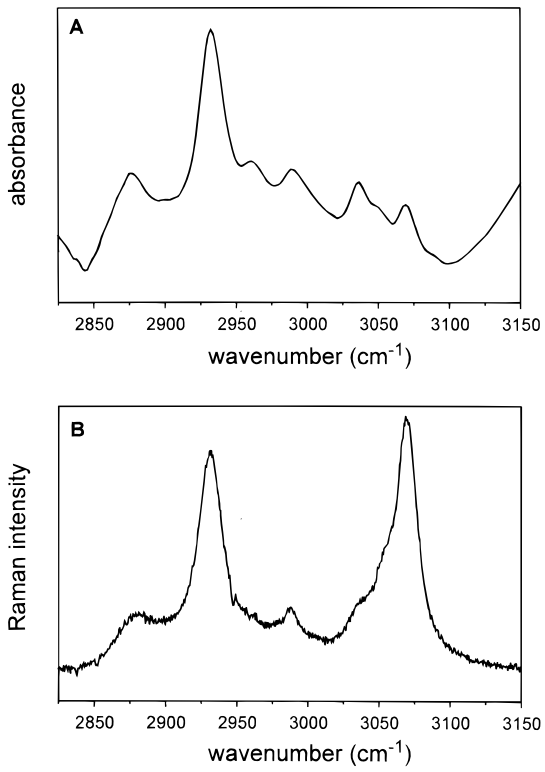

Figure 4. (A) Infrared and (B) Raman spectra of sodium *p*-tosylate (Na hTs) in D_2O in the C−H stretching region. The variable baseline in the infrared spectrum arises from subtraction of the D_2O spectrum.

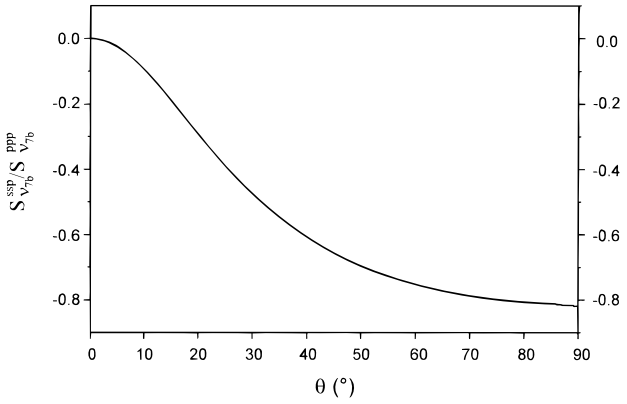

Figure 5. Calculated curve of the relative strength of the ν_{7b} mode in ssp- and ppp-polarized SF spectra as a function of θ. θ is the angle of the C_2 axis of the *p*-tosylate ring with respect to the surface normal of D_2O.

acquired between 2800 and 3100 cm^{-1} at 2 cm^{-1} intervals with 900 laser pulses at each data point. Three sets of ssp- and ppp-polarized spectra were acquired alternately from the surface of one solution. These spectra allowed us to estimate the random error in the ratios of line strengths obtained with the two polarizations. Several other experiments on different samples confirmed the reproducibility of the ssp-, ppp-, and sps-polarized spectra.

Spectra of the surfactant in the C−H stretching region (Figure 8) were obtained from solutions of perprotonated surfactant ($hC_{16}TAB$) and perdeuterated *p*-tosylate (dTs). SF spectra with ssp-polarized beams were acquired between 2800 and 3000 cm^{-1} at 2 cm^{-1} intervals with 1200 laser pulses at each data point. The ssp-polarized spectra were also acquired from solutions containing 1 mM $C_{16}TAB$ and 3 mM NaBr.

The synthesis and purification of $hC_{16}TAB$ and $dC_{16}TAB$ used in these experiments have been described previously.[17b]

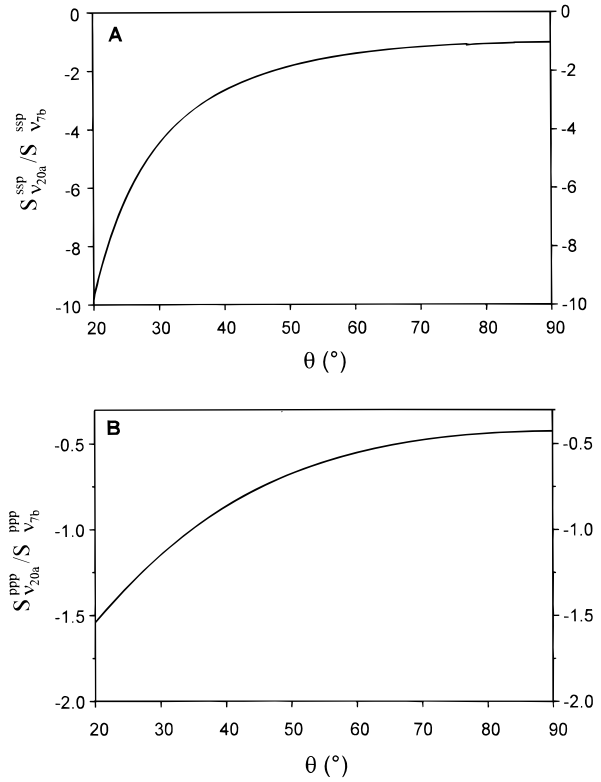

Figure 6. Calculated curves of the relative strength of the ν_{20a} and ν_{7b} modes as a function of θ in (A) ssp- and (B) ppp-polarized SF spectra.

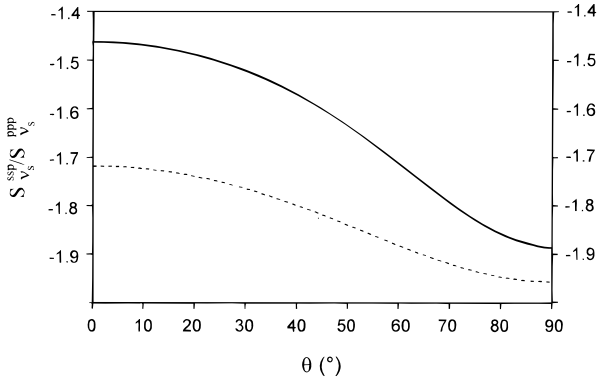

Figure 7. Calculated curves of the relative strength of the symmetric methyl stretching mode ($\nu_s(CH_3)$) in ssp- and ppp-polarized SF spectra as a function of θ. θ is the angle of the C_{3v} axis of the methyl group with respect to the surface normal of D_2O. The curves were calculated with values of r ($=\beta_{aac}/\beta_{ccc}$) of 4 (solid line) and 1.5 (dotted line) and with $n' = 1.40$.

Perdeuterated sodium *p*-tosylate, Na dTs, was synthesized according to literature procedures.[40] Perprotonated sodium *p*-tosylate, Na hTs (Aldrich, 95%), was recrystallized twice from ethanol. D_2O (Fluorochem) was used as received. High-purity H_2O was obtained from an Elga UHQ system.

The SF spectra were fitted with the function $|\sum_v f_v(\omega_{IR}) + S_{NR}e^{i\epsilon}|^2$ where S_{NR} and ϵ model the strength and phase, respectively, of the nonresonant background from the D_2O subphase,[41] $f_v(\omega_{IR})$ is proportional to $\chi^{(2)}_{ijk,R}$, and the summation is over all the resonances in the spectrum. We model $f_v(\omega_{IR})$ for each resonance with a Voigt-like function obtained by convolution of a Lorentzian, $S_v/(\omega_v - \omega_{IR} - i\Gamma_v)$, where S_v is the line strength and Γ_v is the homogeneous line width of the resonance, with a Gaussian distribution of resonant frequencies centered on ω_v with a width σ_v. To fit the spectra, S_v, ω_v, and σ_v were optimized for each resonance. In these spectra, it is difficult to separate the homogeneous and inhomogeneous contributions to the line width so Γ_v was constrained nominally to 2 cm^{-1} for each resonance and only σ_v allowed to vary.

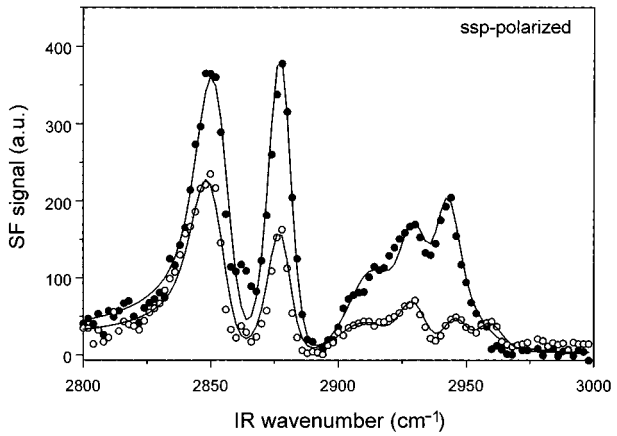

Figure 8. The ssp-polarized SF spectra of surfaces of solutions containing 1 mM $hC_{16}TAB$ and 3 mM NaBr (filled circles) and 3 mM deuterated *p*-tosylate (Na dTs; open circles) in D_2O. The solid lines are computer fits to the spectra.

TABLE 1: Assignments of the Resonances in the SF Spectra of *p*-Tosylate Bound to a Monolayer of $C_{16}TA^+$ [a]

wavenumber/cm^{-1}				
SFS	Raman	IR	ab initio	assignmt
3057	3069	3069	3413 (×2)	$\nu_2 + \nu_{20b}$
3035	3050	3050	3372	ν_{7b}
3021	3037	3036	3372	ν_{20a}
~2990	2988	2990	3292	$\nu'_\alpha(CH_3)$
~2950	~2963	2962	3268	$\nu''_\alpha(CH_3)$
2921	2932	2932	3209	$\nu_s(CH_3)$
2863	2878	2876		$2 \times \delta_{as}$

[a] The vibrational wavenumbers of the modes in the IR and Raman spectra of sodium *p*-tosylate in D_2O are given, as are wavenumbers from the ab initio calculation on *p*-toluenesulfonic acid (see text).

An IR spectrum of a 1 M solution of *p*-tosylate in D_2O was acquired on a Biorad FTS-40 spectrometer, with 64 scans at a resolution of 4 cm^{-1} and a path length of 50 μm. The reference signal from pure D_2O was subtracted from the sample spectrum. The spectrum was fitted with mixed Gaussian/Lorentzian peaks. The IR transition dipole moment is proportional to the square root of the integrated area of a peak. A Raman spectrum at the same concentration was acquired on a Dilor Labram confocal Raman spectrometer. A low-magnification (×10) objective was used to limit the numerical aperture of the incident and collected light so that the scattering angle was close to 180°. The incident He−Ne laser was unpolarized, and the spectrometer was not equipped with a polarizer. The ratio of the polarizabilities of aromatic modes of A_1 and B_1 symmetry can be determined from the peaks areas in the Raman spectrum.[42]

To aid the assignment of the SF spectra, HF−SCF calculations were carried out on *p*-toluenesulfonic acid with the CADPAC program.[43] The large size of the molecule necessitated a relatively simple basis set, 6-31G*. The calculations were carried out using a molecular geometry with one of the C−H bonds of the methyl group oriented perpendicular to the plane of the aromatic ring. The normal modes were computed within the harmonic approximation, which excludes Fermi resonances. It is well-known that SCF calculations overestimate vibrational frequencies by about 10%,[44] which is observed in the frequencies reported in Table 1. The relative ordering of the modes is, however, generally reliable. The dipole moment derivatives and polarizability derivatives generated by the ab

initio calculation did not predict correctly the relative intensities of different modes in the IR and Raman spectra of *p*-tosylate and cannot therefore be used with confidence to calculate the components of the hyperpolarizability: even with larger basis sets it is difficult to represent charge distributions correctly in SCF calculations.

4. Results and Discussion

4.1. SF Spectra of *p*-Tosylate. The counterions associated with the $C_{16}TA^+$ monolayer can be divided into two categories. First, there are those counterions that are specifically associated with the monolayer and are considered as being "bound". The counterion−surfactant interaction may be strong enough to result in a preferred orientation of these counterions. The remainder of the counterions reside in the diffuse double layer. The SF spectra of *p*-tosylate arise only from the "bound" counterions: the strong electric fields existing in the diffuse double layer might, in principle, orient dipolar molecules in the solution, but previous attempts to observe a SF signal from probe molecules with large dipoles in the double layer of a monolayer of a charged surfactant were unsuccessful.[12]

Figure 3 shows the ssp-, ppp-, and sps-polarized SF spectra of a monolayer of $dC_{16}TAB$ in the presence of *p*-tosylate ions. The surfactant was fully deuterated so only the vibrational modes of *p*-tosylate ions appear in the spectra. The *p*-tosylate resonances are convoluted with a weak background signal from the D_2O. In the ssp-polarized spectrum (Figure 3A), interference between the two signals is constructive on the low-frequency side of the major peaks and destructive on the high-frequency side, giving rise to the asymmetric peak shapes. In the ppp-polarized spectrum (Figure 3B), the line strengths are of opposite sign, and constructive interference now occurs on the high-frequency side of the peaks, changing the shape and apparent peak positions. Computer modeling of the SF spectra, however, yielded the same peak frequencies for both polarizations to within 3 cm^{-1}. The sps-polarized spectrum (Figure 3C) is weak, and features are broad and ill-defined. It was not possible to fit this spectrum with any confidence.

Assignment of SF Spectra. Infrared and Raman spectra of sodium *p*-tosylate in D_2O were recorded to aid the assignment of the SF spectra, and they are shown in Figure 4. The aliphatic and aromatic modes of *p*-tosylate that appear in the vibrational spectra between 2800 and 3100 cm^{-1} are shown in Figure 2. The strong peak at 2932 cm^{-1} in the IR and Raman spectra is assigned to the symmetric methyl stretching mode ($\nu_s(CH_3)$) by comparison with the known spectra of toluene.[45] The two peaks in the IR spectrum of *p*-tosylate at 2990 and 2962 cm^{-1} are assigned to the antisymmetric CH_3 stretches, $\nu_a(CH_3)$. The high-frequency component is well-resolved in the Raman spectrum while the low-frequency component appears as an unresolved shoulder in the high-frequency wing of the $\nu_s(CH_3)$ mode. The broad peak near 2877 cm^{-1} in the IR and Raman spectrum is assigned to an overtone of the degenerate bending mode of the methyl group ($2 \times \delta_a$).[45] This mode borrows intensity from the $\nu_s(CH_3)$ mode through a Fermi resonance. Both the IR and Raman spectra indicate the presence of other, weak peaks contributing to a broad background intensity in the 2850−3020 cm^{-1} region, probably from overtone and combination bands. The SF spectra show two principal peaks in the aliphatic C−H stretching region, at 2921 and 2863 cm^{-1}, which we therefore assign to the $\nu_s(CH_3)$ mode and its Fermi resonance. The SF frequencies of tosylate in the monolayer are red-shifted by 10−15 cm^{-1} from the corresponding IR and Raman frequencies in D_2O (Table 1). To fit the high-wavenumber side of the $\nu_s(CH_3)$ resonance in the SF spectra, we needed to include the antisymmetric methyl stretching modes. These peaks are weak, and the wavenumbers from the fitting routine are consequently approximate.

In the aromatic region, the strong peak in the Raman spectrum at 3069 cm^{-1} is conventionally assigned to the ν_2 mode[45] in which all four C−H bonds vibrate in phase (Figure 2B). The two strongest peaks in IR spectra of para-disubstituted benzene rings are normally assigned to the two ν_{20} modes; indeed, for identical substituents these are the only modes with any IR activity. Thus, we are led to assign the two peaks in the IR spectrum of *p*-tosylate at 3036 and 3069 cm^{-1} to the ν_{20} modes. The coincidence between the ν_2 mode and one of the ν_{20} modes is supported by the ab initio calculation, which places the ν_2 and ν_{20b} modes at the same frequency (Table 1). The ν_{20a} mode is also observed in the Raman spectrum at 3037 cm^{-1}. Bearing in mind the red shift observed in the methyl modes, we assign the strong peak in the ssp-polarized SF spectrum at 3057 cm^{-1} to a superposition of the ν_2 and ν_{20b} modes and the weaker peak at 3021 cm^{-1} to the ν_{20a} mode. The observed separation between the two peaks is in agreement with the IR and Raman spectra and the ab initio calculation. To a casual inspection, there are only two peaks in the SF spectrum between 3000 and 3100 cm^{-1}, but to fit the ssp spectrum we needed to include an additional resonance at 3035 cm^{-1} with a negative line strength. We have argued previously that the line strengths of the ν_2 and ν_{7b} modes have opposite signs in ssp-polarized spectra.[11] The ν_{7b} mode is observed in the IR spectrum of *p*-tosylate in D_2O at 3050 cm^{-1} and in the Raman spectrum as a shoulder at 3052 cm^{-1}, on the low-frequency side of the main ν_2 peak. We therefore assign the resonance at 3035 cm^{-1} to the ν_{7b} mode. The assignment of the resonances in the SF, IR, and Raman vibrational spectra of *p*-tosylate is summarized in Table 1.

Determination of the Polar Orientation of the Counterion. If the orientation of a molecule is inverted, $\chi^{(2)}$ changes sign, and consequently, the phase of the emitted SF light changes by π. The phase of emitted light, and hence the polar orientation of a molecule, can be determined either from the interference with the SF light emitted from an external reference, such as quartz, or from a reference signal within the sample. In our previous work on surfactants adsorbed at the interface between water and hydrophobic gold, the strong nonresonant signal from the gold substrate provided such an internal reference.[8,10,11] The shape of resonances associated with vibrations in molecules adsorbed at a gold substrate is determined largely by the interference between the nonresonant and resonant terms. As a consequence, the effect of inverting a molecule on the SF spectrum is dramatic. For example, if a methyl group is oriented away from the gold surface, the $\nu_s(CH_3)$ mode appears as a peak due to constructive interference with the nonresonant signal.[8,11] If the methyl group is oriented toward the gold surface, the interference is destructive, and the $\nu_s(CH_3)$ mode appears as a dip below the level of the nonresonant background signal. From the appearance of the SF spectra of *p*-tosylate bound to a monolayer of $C_{14}TAB$ at the surface of gold, we deduced that the bound tosylate ions were oriented with their aromatic rings away from the aqueous phase.[11]

The nonresonant background due to the D_2O subphase in the SF spectra presented here is much smaller than from gold but is large enough to distort significantly the line shapes in the SF spectra. For both ssp- and ppp-polarizations, the phase of the $\nu_s(CH_3)$ mode of *p*-tosylate relative to the nonresonant background is the same as in a wide range of surfactants at the air−water interface,[46] including densely packed monolayers such

as dodecanol.[9,47] It is well-established that these surfactants are oriented at the air−water interface with their methyl groups pointing away from the aqueous phase:[47] we infer that the methyl groups in the *p*-tosylate ions detected by SFS are also oriented away from the water.

The polar orientation of the counterions provides an indication that the aromatic rings of the *p*-tosylate ions are likely to lie in the hydrophobic region of the monolayer. The frequencies of the resonances in the SF spectra also suggest that the environment of the *p*-tosylate ions in the monolayer is more like a liquid hydrocarbon than water. The SF frequencies are red-shifted by 10−15 cm^{-1} from the IR and Raman frequencies of *p*-tosylate ions dissolved in water with the result that the $\nu_s(CH_3)$ and ν_2 bands in the SF spectra occur at almost the same frequencies as the corresponding IR bands of liquid toluene. These qualitative indications of the position of the bound counterions are supported by quantitative measurements by neutron reflection reported in the following paper.[5]

Determination of the Tilt of the Counterion. To analyze the orientation of the *p*-tosylate ions, we make the reasonable assumption that the Euler angles ϕ and ψ are randomly distributed and the artificial assumption that the tilt, θ, has a δ-function distribution. A Gaussian distribution of angles was considered explicitly in our previous work on benzoate.[14] As the following discussion will show, there are sufficient other uncertainties in the calculation of the tilt that the use of more complex (and more realistic) distributions to refine the determination of the tilt is not justified. The relative intensity of different modes within a SF spectrum, or of the same mode in SF spectra acquired with different polarizations, is determined by the orientation of the ions, the local refractive index, n', of the monolayer, and the hyperpolarizabilities of the vibrational modes (eqs 2 and 6). To calculate the Fresnel coefficients, *K* and *L*, we have assumed that $n' = 1.40$ and that local field corrections are isotropic and therefore cancel in the ratio of line strengths. This value of n' is realistic for a liquid hydrocarbon environment and gave reasonable agreement in a previous study of benzoate ions bound to a monolayer of a cationic surfactant.[14] If we know the components of β, we can then calculate the line strengths, *S*, as a function of θ and, by comparison with experiment, determine θ.

The components of β for different modes can, in principle, be determined from IR and Raman spectra or calculated ab initio. The values of the dipole moment and polarizability derivatives produced by our ab initio calculation on *p*-toluenesulfonic acid did not predict correctly the relative intensities of either the aliphatic or the aromatic resonances in the IR and Raman spectra of *p*-tosylate. It would therefore be imprudent to use the ab initio values of β in quantitative calculations, and we must rely on values determined experimentally. Polarizability and dipole moment derivatives determined from Raman and IR spectra are, however, subject to uncertainty and error. We therefore present analyses of the modes in descending order of confidence in the hyperpolarizability values.

We consider first the ν_{7b} mode at 3035 cm^{-1}. For modes of B_1 symmetry, only $\beta_{aca} = \beta_{caa}$ is nonzero: the relative intensity of the ν_{7b} mode in the ssp- and ppp-polarized spectra is therefore independent of the value of the hyperpolarizability. Since the ν_{7b} mode is weak and overlaps the ν_2 and ν_{20a} modes, it is difficult to assign a precise value to its line strength. We are, however, confident that $S^{ssp}_{\nu_{7b}}/S^{ppp}_{\nu_{7b}}$ lies in the range −0.4 to −0.7. Figure 5 shows the simulated curve of $S^{ssp}_{\nu_{7b}}/S^{ppp}_{\nu_{7b}}$ against θ calculated from eqs 6 and 7. Comparison of the calculated curve with the experimental value of $S^{ssp}_{\nu_{7b}}/S^{ppp}_{\nu_{7b}}$ yields a mean tilt in the range $25° < \theta < 50°$.

We next consider the ν_{20a} mode. For the aromatic modes of A_1 symmetry only β_{aac}, β_{bbc}, and β_{ccc} are nonzero. Furthermore, as the polarizability derivative perpendicular to the aromatic ring is much smaller than in the plane of the ring, $S^{ssp}_{\nu_{20a}}/S^{ppp}_{\nu_{20a}}$ depends only on the relative magnitude of β_{ccc} and β_{aac}. Equation 3 shows that β_{ccc}/β_{aac} is equal to the anisotropy in the Raman tensor: $\alpha'_{cc}/\alpha'_{aa} = t$. Experimental values of $\alpha'_{cc}/\alpha'_{aa}$ for the ν_{20a} mode do not exist for *p*-tosylate and would be difficult to obtain due to overlap with the ν_2 and ν_{7b} bands. If we assume bond additivity of the polarizability derivatives, we can predict values of $\alpha'_{cc}/\alpha'_{aa}$ for a para-disubstituted benzene ring from the Raman tensor of the ν_2 and ν_{7a} modes of benzene. Experimental Raman measurements by Fernandez-Sanchez and Montero[48] lead to an estimate of $t = \alpha'_{cc}/\alpha'_{aa} = 0.38$ for a para-disubstituted ring; ab initio calculations on benzene by Goodman[49] at the 6-311++G(d,p) level produce a similar value of $t = \alpha'_{cc}/\alpha'_{aa} = 0.42 \pm 0.08$. If we use a value of $\beta_{ccc}/\beta_{aac} = 0.40$, we find that the value of $S^{ssp}_{\nu_{20a}}/S^{ppp}_{\nu_{20a}}$ calculated from eqs 6 and 7 is almost independent of tilt, ranging from −1.8 to −1.9. The experimental value of $S^{ssp}_{\nu_{20a}}/S^{ppp}_{\nu_{20a}}$ is -2 ± 0.2. While the comparison between calculated and experimental values of $S^{ssp}_{\nu_{20a}}/S^{ppp}_{\nu_{20a}}$ tells us nothing about the tilt, the agreement obtained does lead to increased confidence that our analytical approach and the assumptions therein are broadly correct.

The relative intensity of the ν_{20a} and ν_{7b} modes in ssp- and ppp-polarized spectra is much more sensitive to the tilt of the *p*-tosylate. If we assume a value of $t = \alpha'_{cc}/\alpha'_{aa} = 0.40$ for the ν_{20a} mode, we can estimate the ratio of $\alpha'_{cc}(\nu_{20a})/\alpha'_{ac}(\nu_{7b})$ from the isotropic Raman spectrum of *p*-tosylate.[42] The ratio of $\mu'_c(\nu_{20a})/\mu'_a(\nu_{7b})$ can be estimated from the IR spectrum. While band overlap inevitably introduces some uncertainty into these estimates, we can nevertheless obtain an approximate experimental value of $\beta_{ccc}(\nu_{20a})/\beta_{aca}(\nu_{7b}) = 1.15$. This ratio is slightly higher than that calculated ab initio (0.92). Figure 6 shows the ratios $S^{ssp}_{\nu_{20a}}/S^{ssp}_{\nu_{7b}}$ and $S^{ppp}_{\nu_{20a}}/S^{ppp}_{\nu_{7b}}$, predicted from eqs 6 and 7, as a function of θ for $t = \beta_{ccc}(\nu_{20a})/\beta_{aac}(\nu_{20a}) = 0.4$ and $\beta_{aac}(\nu_{20a})/\beta_{aca}(\nu_{7b}) = 1.15$. $S^{ssp}_{\nu_{20a}}/S^{ssp}_{\nu_{7b}}$ is independent of Fresnel factors and will therefore be less prone to error than $S^{ppp}_{\nu_{20a}}/S^{ppp}_{\nu_{7b}}$, which depends on the value assumed for the local refractive index of the monolayer. Computer fitting of the SF spectra yielded values of $S^{ssp}_{\nu_{20a}}/S^{ssp}_{\nu_{7b}} = -3.3 \pm 0.7$ and $S^{ppp}_{\nu_{20a}}/S^{ppp}_{\nu_{7b}} = -0.9 \pm 0.2$. Comparison of the experimental line strengths with the calculated values (Figure 6) yields a mean tilt of $36 \pm 3°$ for both polarizations.

Many authors have used the intensity of the $\nu_s(CH_3)$ mode in SF spectra to calculate the tilt of the methyl group.[47,50−52] Most have used the ratio intensities of the $\nu_s(CH_3)$ in the ssp- and sps-polarized spectra. In the sps-spectrum of *p*-tosylate (Figure 3C), the $\nu_s(CH_3)$ mode is weak and overlaps other modes, making it difficult to calculate the tilt quantitatively by this method. We therefore focus our attention on the ratio of strengths in the ssp- and ppp-polarized spectra. We find experimentally that $S^{ssp}_{\nu_s}/S^{ppp}_{\nu_s} = -1.5 \pm 0.1$. The error limits represent the range of ratios obtained in three sets of measurements and give an indication of the reproducibility of the experiment and of random fitting errors. The limits do not allow for systematic errors in the fitting procedure associated with, for example, the treatment of the overlapping antisymmetric stretching modes.

The $\nu_s(CH_3)$ mode has invariably been analyzed with the assumption of C_{3v} symmetry. This assumption is invalid for *p*-tosylate, despite the fact that the methyl group is freely rotating

(the barrier to internal rotation in toluene is only 4.88 cm^{-1}).[53] The true symmetry is either C_1 or C_s, depending on the torsional angle. After averaging over torsional angles, only components of β that are nonzero in the C_{2v} point group remain. Ab initio calculations show that $\beta_{aca} = \beta_{caa}$ and $\beta_{bcb} = \beta_{cbb}$ are much smaller than β_{ccc}, β_{aac}, and β_{bbc} and can therefore be ignored. There is no reason β_{aac} and β_{bbc} should be equal; indeed, in the ab initio calculation they differed by a factor of 2. However, if one assumes random twists about the *c*-axis, then the methyl group can be analyzed as if it had C_{3v} symmetry, with β_{aac} and β_{bbc} given by the arithmetic mean of the true values. To analyze the polarized SF spectra, only the ratio $r = (\beta_{bbc} + \beta_{aac})/2\beta_{ccc} = (\alpha'_{aa} + \alpha'_{bb})/2\alpha'_{cc}$ needs to be determined. For molecules with C_{3v} symmetry it can be shown that r is equal to the ratio $(\langle\beta_{xxz}\rangle - \langle\beta_{xzx}\rangle)/(\langle\beta_{zzz}\rangle + 2\langle\beta_{xzx}\rangle)$, but problems in fitting the sps-polarized spectrum hinders determination of r by this route. Various values of r have been used in the past to analyze SF spectra: $r = 4$ (only the polarizability derivative along the C−H bond is nonzero),[51] 3.4 (from the depolarization ratio,[54] ρ, of ethanol),[47] and 1.7 (from ρ of methanol).[52] Experimental measurements of ρ in ethane yielded a lower value of $r = 1.41$,[55] and theoretical calculations on the same molecule gave $r = 1.57$.[56] Gough has shown from calculations on various hydrocarbons that the anisotropy in the Raman tensor of the methyl group is a nonlocal property and that the principal axes of the Raman tensor do not necessarily coincide with the symmetry axes of the methyl group.[56] Given that the value of r for the $\nu_s(CH_3)$ mode cannot be determined from ρ in molecules that do not have C_{3v} symmetry, even if experimental data of sufficient accuracy exist, and that polarizability derivatives may not be transferable, there clearly remains considerable uncertainty in the correct value of r to employ, even within the assumed model of C_{3v} symmetry. We have therefore analyzed the SF spectra with a range of values of r between 4 and 1.5.

Figure 7 shows the calculated ratio $S^{ssp}_{\nu_s}/S^{ppp}_{\nu_s}$ as a function of θ for $r = 4$ and for $r = 1.5$. For $r = 4$ (the highest plausible value based on a bond additivity model), the calculated curve yields a mean tilt of 30° with upper and lower limits of 0° and 45° given by the error in $S^{ssp}_{\nu_s}/S^{ppp}_{\nu_s}$. Reducing the value of r yields a lower tilt; however, at values lower than 2 there is no agreement between the calculated and experimental values. For example, the calculated curve with $r = 1.5$ is insensitive to θ, and no orientation is consistent with the experimental value of $S^{ssp}_{\nu_s}/S^{ppp}_{\nu_s} = -1.5 \pm 0.1$.

Next we consider the strong peak at 3057 cm^{-1} in the SF spectra (Figure 3A,B). The dominant contribution to this peak is the ν_2 mode, but as discussed above, it also contains a contribution from the ν_{20b} mode. An analysis based on the ν_2 mode alone parallels exactly that of the ν_{20a} mode (since the "pure" ν_{20a} mode gains Raman intensity by mixing with the ν_2 mode) and therefore yields values of S^{ssp}/S^{ppp} in the region of −2 for $\beta_{ccc}/\beta_{aac} \sim 0.4$, independent of tilt. Fitting of the peak at 3057 cm^{-1} yields a ratio of line strengths of -2.8 ± 0.3, which is inconsistent with an analysis based solely on the ν_2 mode. To incorporate the effects of the ν_{20b} mode, we need to know the relative values of the hyperpolarizabilities of the two modes. The coincidence of the two vibrational frequencies, however, prevents us from determining the IR and Raman cross sections individually. We are therefore left in the unsatisfactory position that the most intense aromatic peak in the spectrum defies quantitative analysis. If we use the value of $\beta_{aca}(\nu_{20b})/\beta_{aac}(\nu_2) = 0.4$ returned by the ab initio calculation, the experimental data are consistent with a tilt of approximately 35°. Given the uncertainty over the accuracy of the hyperpolarizabilities calculated ab initio, however, the agreement with the tilt estimated from other bands must be considered fortuitous.

The preceding discussion illustrates the difficulties inherent in a quantitative analysis of the SF spectra. Although the tilt angle from any single comparison is subject to considerable uncertainty, the broad agreement between the tilt angles determined from the analysis of several modes (ν_{7b}, ν_{20a}, and $\nu_s(CH_3)$) inspires greater confidence in the results of those analyses. On this basis, we would suggest that a mean tilt of 30−40° is most likely for the *p*-tosylate ions bound to the $C_{16}TA^+$ monolayer. To put this value into context, it is useful to draw a comparison with recent molecular dynamics simulations of phenol at the air−water interface.[57] The distribution of phenol orientations was peaked at $\theta = 0°$ but was very broad with a value of $\langle\cos\theta\rangle = 0.6$ at coverages comparable to those in our experiments. The equivalent "tilt" from the surface normal (defined here as the inverse cosine of $\langle\cos\theta\rangle$) is 53°. For a random distribution of angles in the upper half-plane, $\langle\cos\theta\rangle = 0.5$ and $\theta = 60°$. In comparison, the *p*-tosylate ions bound to a $C_{16}TA^+$ monolayer are much less tilted. A previous study of benzoate ions bound to a monolayer of a $C_{14}TA^+$ at the air−water interface also concluded that the bound counterions were oriented close to the surface normal.[14]

4.2. SF Spectra of C_{16}TAB in the Presence of Deuterated *p*-Tosylate. We now turn our attention to the SF spectra of the $C_{16}TA^+$ ions at the air−water interface. Figure 8 shows the ssp-polarized spectra from the surface of a 1 mM solution of hC_{16}TAB in the presence of either 3 mM NaBr or 3 mM Na dTs, together with computer fits to the spectra. These spectra show the effect of *p*-tosylate ions on the structure of the surfactant monolayer. The control spectrum in the absence of *p*-tosylate was acquired in the presence of 3 mM NaBr so that the ionic strength was held constant.

The assignments of the peaks in the SF spectra of this surfactant are well established.[8] The two peaks at 2878 and 2942 cm^{-1} are assigned to a Fermi resonance between the symmetric stretch of the methyl group and overtones of the antisymmetric bending modes (labeled $r^+$and r^+_{FR}, respectively). The antisymmetric methyl stretching mode (r^-) appears as an unresolved shoulder near 2960 cm^{-1}. Signal from the methylene modes of the surfactant appears at 2850 cm^{-1} and in the range 2900−2930 cm^{-1}. The lower frequency peak is assigned to the symmetric methylene stretching mode (d^+) and the higher frequency region to combinations of methylene deformation modes in Fermi resonance with the d^+ mode (d^+_{FR}). The antisymmetric methylene stretch (d^-) expected around 2925 cm^{-1} is not clearly resolved from the d^+_{FR} mode. We fitted the d^+_{FR} mode with two broad resonances centered at 2915 and 2930 cm^{-1}, though this choice of parameters is somewhat arbitrary. The SF spectrum of dC_{16}hTAB showed no discernible peaks from the trimethylammonium group in this spectral region.

The r^+ and d^+ modes are well-resolved and can be fitted with confidence. The relative line strengths of these two modes, $S^{ssp}_{r^+}/S^{ssp}_{d^+}$, is a sensitive measure of conformational disorder in the hydrocarbon chains; the line strength of the r^+ mode by itself provides a measure of the orientation of the terminal methyl groups. The line strengths of these modes from the fits in Figure 8 are shown in Table 2. If we assume that the local field corrections are the same in each monolayer, then the line strengths are proportional to $N\langle\beta\rangle$. To separate the effects of number density and orientation on the SF spectra, we multiply the line strengths by the area per molecule ($A = N^{-1}$) determined by neutron reflection (see following paper).[5] These normalized

TABLE 2: Line Strengths (au) in SF Spectra Normalized by the Surface Excess, $N = A^{-1}$, for the Symmetric Methyl (r^+) and Methylene (d^+) Modes of $HC_{16}TAB$ in the Presence of Added Salt

	$S^{ssp}_{r^+}A$/nm^2	$S^{ssp}_{d^+}A$/nm^2	$S^{ssp}_{r^+}/S^{ssp}_{d^+}$
$hC_{16}TAB$ + 3 mM NaBr	29	32	0.92
$hC_{16}TAB$ + 3 mM NadTs	21	31	0.68

line strengths (Table 2) are determined by conformation and orientation alone.

At present we are only able to provide a qualitative interpretation of the intensity of the d^+ mode. The methylene groups in an all-trans hydrocarbon chain are locally centrosymmetric. The normal modes of the CH_2 groups in an all-trans chain are therefore either IR- or Raman-active, but not both (the rule of mutual exclusion), and are consequently SF-inactive. As a result of end effects, even an all-trans chain in a surfactant is not exactly centrosymmetric: the methylene group adjacent to the methyl terminus gives rise to a weak peak (d^+_ω) near 2965 cm^{-1}.[58] This peak is clearly seen in the SF spectrum of $C_{16}TAB$ in Figure 8 (filled circles) in which the computer fit excluded the d^+_ω mode. The main d^+ peak at 2850 cm^{-1}, however, is assigned to gauche defects that break the symmetry of the hydrocarbon chain and is virtually nonexistent in densely packed monolayer assemblies. The d^+ mode is therefore a good qualitative indicator of conformational disorder. The normalized intensity of the d^+ mode, $S^{ssp}_{d^+}A$, in the spectra of $C_{16}TAB$ is the same in the presence of either NaBr or Na dTs (Table 2), which suggests that incorporation of *p*-tosylate ions in the monolayer does not greatly alter the number of conformational defects in the monolayer.

The intensity of the mode can be related quantitatively to tilt angle. To a good approximation, $S^{ssp}_{r^+}$ is proportional to $\langle\cos\theta\rangle$, if C_{3v} symmetry is assumed.[59] The true local symmetry is C_s, but chain disorder will lead to a wide range of orientations of the mirror plane; consequently, an analysis based on the assumption of C_{3v} symmetry is likely to be a good approximation. A further issue in the interpretation of the line strength is that a variety of different models can give the same value for $\langle\cos\theta\rangle$. For example, $\langle\cos\theta\rangle = 0.5$ could reflect a constant angle $\theta = 60°$ between the surface normal and the *c*-axis of the methyl group, a random distribution of angles in the upper half-plane, or a uniform chain tilt $\chi = 52°$. The first of these models is unreasonable for a disordered monolayer: the true distribution probably lies between the other two extremes. For comparative purposes, the third model is the most useful; i.e., we assume that the axis of the chain near the methyl terminus is uniformly tilted but that there is no preferred twist about that axis: the methyl group axes are randomly distributed on a cone of half-angle 35° about the chain director. To calculate the chain tilt, we use the intensity of the mode in a monolayer of dodecanol, for which $\chi \sim 0°$, as a reference. SF spectra of dodecanol were not recorded at the same time as the spectra of reported here, but the necessary comparisons can be drawn from sets of spectra acquired on other occasions. We find that the normalized strength of the r^+ mode (Table 2) relative to that of dodecanol is 0.5 for $C_{16}TAB$ and 0.36 for $C_{16}TA^+Ts^-$. The corresponding chain tilts are $58 \pm 4°$ and $67 \pm 3°$, respectively, where the errors are nominal estimates based on a 10% error in the normalization procedure.[60] We infer that the ends of the hydrocarbon chains are tilted further away from the surface normal in the presence of *p*-tosylate. These data make sense in the context of an overall model for the surfactant monolayer, which is discussed after presentation of the neutron reflection data in the accompanying paper.[5]

5. Conclusions

The observation of SF vibrational spectra of *p*-tosylate ions in monolayers of $C_{16}TA^+Ts^-$ at the surface of D_2O indicates that at least some of the bound ions have a preferred orientation. The phase of the symmetric methyl stretching mode of *p*-tosylate ions shows that the ions are oriented with the methyl groups away from the aqueous subphase; a red shift in the frequencies of the vibrational resonances of *p*-tosylate is consistent with the ions residing in a nonpolar environment such as might be found in the interior of the monolayer. The relative intensities of the aliphatic and aromatic C−H stretching modes in polarized SF spectra suggest that the C_2 axis of the *p*-tosylate ions is tilted on average by 30−40° from the surface normal.

The vibrational spectra of the adsorbed surfactant molecules indicated that there was little change in the number of gauche defects when *p*-tosylate was bound to the monolayer. However, the change in the strength of the symmetric stretch of the terminal methyl groups showed that the chain termini were tilted further from the surface normal (by about 9°) when *p*-tosylate was bound to the monolayer. The mean tilt of the ends of the hydrocarbon chains of the surfactant molecules (60−70°) is much greater than the tilt of the *p*-tosylate ions.

This study of *p*-tosylate ions highlights the difficulties that still remain in the quantitative analysis of SF spectra of large or complex molecules. Ab initio calculations will undoubtedly become a valuable resource to support such analyses, but independent checks, such as IR and Raman spectra, are still required to assess the accuracy of calculated hyperpolarizabilities. We, and others, have used experimental measurements of Raman depolarization ratios as a means of reducing the number of unknown components of the hyperpolarizability. Experimental values of ρ rarely exist for the molecule under study, and a wide range of values of ρ can be found depending on the molecule chosen as a representative comparison. Raman depolarization measurements can also not distinguish between r and r^{-1} or provide useful information for modes where there are more than two independent components of the Raman tensor. Given the ambiguities in both experimental Raman depolarization ratios and ab initio calculations, careful consideration has to be given to the choice of values in the hyperpolarizability tensors used to analyze SF spectra.

Acknowledgment. This work was supported by the EPSRC and Unilever Research Port Sunlight Laboratory. D.C.D. thanks Emmanuel College, Cambridge (U.K.), for a Research Fellowship. We thank D. Borst (Pittsburgh University) for making available to us the results of his ab initio calculations on toluene and T. Greene (Oxford University) for assistance in acquiring the Raman spectrum.

References and Notes

(1) (a) Evans, D. F.; Wennerström, H. *The Colloidal Domain*; VCH: New York, 1994. (b) Zana, R. In *Cationic Surfactants-Physical Chemistry*; Rubingh, D. N., Holland, P. M., Eds.; Dekker: New York, 1991; p 41. (c) Lindman, B.; Wennerström, H. *Top. Curr. Chem.* **1980**, *87*, 1−83.

(2) Gravsholt, S. *J. Colloid Interface Sci.* **1976**, *57*, 575−577.

(3) Rehage, H.; Hoffmann, H. *Faraday Discuss. Chem. Soc.* **1983**, *76*, 363−373. Hoffmann, H.; Rehage, H.; Reizlein, K.; Thurn, H. *ACS Symp. Ser.* **1985**, *272*, 41−66. Shikata, T.; Dahman, S. J.; Pearson, D. S. *Langmuir* **1994**, *10*, 3470−3476.

(4) (a) Hoffmann, H. *Adv. Mater.* **1994**, *6*, 116−129. (b) Hoffmann, H.; Ebert, G. *Angew. Chem., Int. Ed. Engl.* **1988**, *27*, 902−912. (c) Hoffmann, H. *ACS Symp. Ser.* **1994**, *578*, 2−31.

(5) Li, Z. X.; Bain, C. D.; Thomas, R. K.; Duffy, D. C.; Penfold, J. *J. Phys. Chem. B* **1998**, *102*, 9473.

(6) Bell, G. R.; Bain, C. D.; Li, Z. X.; Thomas, R. K.; Duffy, D. C.; Penfold, J. *J. Am. Chem. Soc.* **1997**, *119*, 10227−10228.

(7) Shen, Y. R. *Nature* **1989**, *337*, 519−525. Bain, C. D. *J. Chem. Soc., Faraday Trans.* **1995**, *91*, 1281−1296. Eisenthal, K. B. *Chem. Rev.* **1996**, *96*, 1343−1360.

(8) Ward, R. N.; Duffy, D. C.; Davies, P. B.; Bain, C. D. *J. Phys. Chem.* **1994**, *98*, 8536−8542.

(9) Bell, G. R.; Bain, C. D.; Ward, R. N. *J. Chem. Soc., Faraday Trans.* **1996**, *92*, 515−523.

(10) Duffy, D. C.; Ward, R. N.; Davies, P. B.; Bain, C. D. *J. Am. Chem. Soc.* **1994**, *116*, 1125−1126.

(11) Duffy, D. C.; Davies, P. B.; Bain, C. D. *J. Phys. Chem.* **1995**, *99*, 15241−15246.

(12) Duffy, D. C. Ph.D. Thesis, University of Cambridge, 1996.

(13) Duffy, D. C.; Davies, P. B.; Bain, C. D.; Creeth, A. M.; Ward, R. N. *Proc. SPIE* **1995**, *2547*, 342−351.

(14) Ward, R. N.; Duffy, D. C.; Bell, G. R.; Bain, C. D. *Mol. Phys.* **1996**, *88*, 269−280.

(15) Lu, J. R.; Simister, E. A.; Thomas, R. K.; Penfold, J. *J. Phys.: Condens. Matter* **1994**, *6*, A403−A408.

(16) (a) Lyttle, D. J.; Lu, J. R.; Su, T. J.; Thomas, R. K.; Penfold, J. *Langmuir* **1995**, *11*, 1001−1008. (b) Lu, J. R.; Hromadova, M.; Thomas, R. K.; Penfold, J. *Langmuir* **1993**, *9*, 2417−2425. (c) Naumann, C.; Dietrich, C.; Lu, J. R.; Thomas, R. K.; Rennie, A. R.; Penfold, J. *Langmuir* **1994**, *10*, 1919−1925.

(17) (a) Lu, J. R.; Li, Z. X.; Smallwood, J.; Thomas, R. K.; Penfold, J. *J. Phys. Chem.* **1995**, *99*, 8233−8243. (b) Lu, J. R.; Hromadova, M.; Simister, E.; Thomas, R. K.; Penfold, J. *J. Phys. Chem.* **1994**, *98*, 11519−11526.

(18) Anacker, E. W. In *Solution Chemistry of Surfactants*; Mittal, K. L., Ed.; Plenum: New York, 1979; p 247. Porte, G. In *Micelles, Membranes, Microemulsions and Monolayers*; Gelbart, W. G., Ben-Shaul, A., Roux, D., Eds.; Springer: New York, 1994; Chapter 2.

(19) (a) Soltero, J. F. A.; Puig, J. E.; Manero, O.; Schulz, P. C. *Langmuir* **1995**, *11*, 3337−3346. (b) Soltero, J. F. A.; Puig, J. E.; Manero, O. *Langmuir* **1996**, *12*, 2654−2662.

(20) *Structure and Flow in Surfactant Solutions*; ACS Symposium Series 578; Herb, C. A., Prud'homme, R. K., Eds.; American Chemical Society: Washington, DC, 1994.

(21) Tanford, C. *Physical Chemistry of Macromolecules*; Wiley: New York, 1961; Chapter 6,

(22) (a) Smith, B. C.; Chou, L. C.; Lu, B.; Zakin, J. L. *ACS Symp. Ser.* **1994**, *578*, 370−379. (b) Smith, B. C.; Chou, L. C.; Zakin, J. L. *J. Rheol.* **1994**, *38*, 73−83.

(23) See, for example: Nemoto, N.; Kuwahara, M.; Yao, M. L.; Osaki, K. *Langmuir* **1995**, *11*, 30−36. Imae, T.; Kohsaki, T. *J. Phys. Chem.* **1992**, *96*, 10030−10035. Ng, S. C.; Gan, C. M.; Chew, C. H. *Colloid Polym. Sci.* **1992**, *270*, 64−67.

(24) See, for example: Carver, M.; Smith, T. L.; Gee, J. C.; Delichere, A.; Caponetti, E.; Majid, L. J. *Langmuir* **1996**, *12*, 691−698. Imae, T.; Kakitani, M.; Kato, M.; Furusaka, M. *J. Phys. Chem.* **1996**, *100*, 20051−20055. Hoffmann, H.; Kalus, J.; Thurn, H.; Ibel, K. *Ber. Bunsen-Ges. Phys. Chem.* **1983**, *87*, 1120−1129.

(25) Clausen, T. M.; Vinson, P. K.; Minter, J. R.; Davis, H. T.; Talmon, Y.; Miller, W. G. *J. Phys. Chem.* **1992**, *96*, 474−478. Lin, Z.; Cai, J. J.; Scriven, L. E.; Davis, H. T. *J. Phys. Chem.* **1994**, *98*, 5984−5993. Sakaiguchi, Y.; Shikata, T.; Urakami, H.; Tamura, A.; Hirata, H. *Colloid Polym. Sci.* **1987**, *265*, 750−753.

(26) Hirata, H.; Sakaiguchi, Y. *J. Colloid Interface Sci.* **1988**, *121*, 300−301.

(27) Kreke, P. J.; Magid, L. J.; Gee, J. C. *Langmuir* **1996**, *12*, 691−698.

(28) (a) Manohar, C.; Rao, U. R. K.; Valaulikar, B. S.; Iyer, R. M. *J. Chem. Soc., Chem. Commun.* **1986**, 379−381. (b) Rao, U. R. K.; Manohar, C.; Valaulikar, B. S.; Iyer, R. M. *J. Phys. Chem.* **1987**, *91*, 3286−3291.

(29) (a) Bachofer, S. J.; Turbitt, R. M. *J. Colloid Interface Sci.* **1990**, *135*, 325−334. (b) Bachofer, S. J.; Simonis, U.; Nowicki, T. A. *J. Phys. Chem.* **1991**, *95*, 480−488. (c) Bachofer, S. J.; Simonis, U. *Langmuir* **1996**, *12*, 2, 1744−1754.

(30) (a) Olsson, U.; Söderman, O.; Guéring, P. *J. Phys. Chem.* **1986**, *90*, 5223−5232. (b) Broxton, T. J.; Christie, J. R.; Chung, R. P.-T. *J. Org. Chem.* **1988**, *53*, 3081−3084.

(31) (a) Jansson, M.; Stilbs, P. *J. Phys. Chem.* **1987**, *91*, 113−116. (b) Jansson, M.; Li, P.; Stilbs, P. *J. Phys. Chem.* **1989**, *93*, 1448−1451.

(32) Narayanan, J.; Manohar, C.; Langevin, D.; Urbach, W. *Langmuir* **1997**, *13*, 398−401.

(33) (a) Israelachvili, J. N. *Intermolecular and Surface Forces*, 2nd ed.; Academic Press: London, 1991. (b) Israelachvili, J. N.; Mitchell, D. J.; Ninham, B. W. *J. Chem. Soc., Faraday Trans. 1* **1976**, *72*, 1525−1568.

(34) Equation 1 assumes that the electric field is written in the form $\mathbf{E}(r,t) = {}^1/_2(\mathbf{E}_0 e^{i(\mathbf{k}\cdot\mathbf{r}-\omega t)} + \text{c.c.})$. Other definitions of **E** lead to differences of factors of 2 in eq 1. The factor $A\tau \cos\theta_{sum}$ arises from converting the intensity of the SF beam into energy per pulse and the factor $(\hbar\omega_{sum})^{-1}$ from converting energy into photons. Other geometric factors are subsumed within the Fresnel coefficients.

(35) Higher-order multipoles can lead to SF emission from the bulk solution, but these terms are negligible compared to the dipole-allowed signal from the monolayer.

(36) Superfine, R.; Huang, J. Y.; Shen, Y. R. *Chem. Phys. Lett.* **1990**, *172*, 303−306.

(37) Long, D. A. *Raman Spectroscopy*; McGraw-Hill: New York, 1977.

(38) Hirose, C.; Akamatsu, N.; Domen, K. *Appl. Spectrosc.* **1992**, *46*, 1051−1072.

(39) We label the aromatic modes according to the conventions of Wilson (Wilson, E. B. *Phys. Rev.* **1934**, *45*, 706).

(40) Furniss, B. S.; Hannaford, A. J.; Smith, P. W. G.; Tatchell, A. R. *Vogel's Textbook of Practical Organic Chemistry*, 5th ed.; Longman: London, 1989.

(41) Bain, C. D.; Davies, P. B.; Ong, T. H.; Ward, R. N.; Brown, M. A. *Langmuir* **1991**, *7*, 1563−1566.

(42) Under the conditions under which the Raman spectrum of *p*-tosylate was acquired, the scattered Raman intensity is given by (ref 37)

$$ {}^nI(\pi) = k_\nu \nu_0{}^4(\alpha'_{yx}{}^2 + \alpha'_{yy}{}^2 + \alpha'_{xx}{}^2 + \alpha'_{xy}{}^2)I_0 $$

where k_ν is a constant, ν_0 is the frequency of the scattered radiation, α' is the Raman tensor, and I_0 is the intensity of the incident radiation. For freely rotating molecules,

$$ \overline{\alpha'^2_{xy}} = \overline{\alpha'^2_{xy}}\gamma'^2/15 $$

and

$$ \overline{\alpha'^2_{xy}} = \overline{\alpha'^2_{xy}} = (45a'^2 + 4\gamma'^2)/45 $$

where

$$ a' = {}^1/_3(\alpha'_{aa} + \alpha'_{bb} + \alpha'_{cc}) $$

and

$$ \gamma'^2 = {}^1/_2\{(\alpha'_{aa} - \alpha'_{bb})^2 + (\alpha'_{aa} - \alpha'_{cc})^2 + (\alpha'_{cc} - \alpha'_{bb})^2 + 6(\alpha'_{ab}{}^2 + \alpha'_{ac}{}^2 + \alpha'_{bc}{}^2)\} $$

For aromatic modes of B_1 symmetry only $\alpha'_{ac} \neq 0$ and hence

$$ {}^nI(\pi) \propto 7\alpha'_{ac}{}^2/15 $$

For aromatic modes of A_1 symmetry $\alpha'_{aa}, \alpha'_{cc} \gg \alpha'_{bb}$. Letting $\alpha'_{cc}/\alpha'_{aa} = t$, we find that

$$ {}^nI(\pi) \propto \alpha'_{aa}{}^2\{4(1 + t^2)/15 + t/15\} $$

If we assume a value for t, we can then determine $\alpha'_{ac}(\nu_{7b})/\alpha'_{aa}(\nu_{20a})$ from the ratio of peak areas in the isotropic Raman spectrum.

(43) Amos, R. D.; Alberts, I. L.; Andrews, J. S.; Colewell, S. M.; Handy, N. C.; Jayatilaka, D.; Knowles, P. J.; Kobayashi, R.; Laidig, K. E.; Laming, G.; Lee, A. M.; Maslen, P. E.; Murray, C. W.; Rice J. E.; Simandiras, E. D.; Stone, A. J.; Su, M.-D.; Tozer, D. J. *Cambridge Analytic Derivatives Package*, Issue 6; Cambridge University Press: New Yok, 1995.

(44) Radom, L.; Schleyer, P. v. R.; Pople, J. A. *Ab Initio Molecular Orbital Theory*; Wiley: London, 1986.

(45) Fuson, N.; Garrigou-Lagrange, C.; Josien, M. L. *Spectrochim. Acta* **1960**, *16*, 106−127.

(46) For monolayers on H_2O, Richmond has shown that the phase of the nonresonant background depends on the charge of the surfactant (see Gragson, D. E.; McCarty, B. M.; Richmond, G. L. *J. Phys. Chem.* **1996**, *100*, 14272−14275): this phenomenon is not observed in SF spectra of the surface of D_2O, in which the phase is constant.

(47) Braun, R.; Casson, B. D.; Bain, C. D. *Chem. Phys. Lett.* **1995**, *245*, 326−334.

(48) Fernandez-Sanches, J. M.; Montero, S. *J. Chem. Phys.* **1989**, *90*, 2909−2914.

(49) Ozkabak, A. G.; Thakur, S. N.; Goodman, L. *Int. J. Quantum. Chem.* **1991**, *39*, 411−422.

(50) Stanners, C. D.; Du, Q.; Chin, R. P.; Cremer, P.; Somorjai, G. A.; Shen, Y. R. *Chem. Phys. Lett.* **1995**, *232*, 407−413. Hatch, S. R.; Polizzotti, R. S.; Dougal, S.; Rabinowitz, P. *Chem. Phys. Lett.* **1992**, *196*, 97−102. Zhang, D.; Gutow, J. H.; Eisenthal, K. B.; Heinz, T. H. *J. Chem. Phys.* **1993**, *98*, 5099−5101.

(51) Guyot-Sionnest, P.; Hunt, J. R.; Shen, Y. R. *Phys. Rev. Lett.* **1987**, *59*, 1597−1600.

(52) Wolfram, K.; Laubereau, A. *Chem. Phys. Lett.* **1994**, *228*, 83−88.
(53) Rudolph, H. D.; Dreizler, H.; Jaeschke, A.; Wendling, P. *Z. Naturforsch.* **1967**, *22A*, 940.
(54) Even here there is an ambiguity since ρ is the same for r and r^{-1}, and one must therefore argue on other grounds which component of α' is the larger.
(55) Martin, J.; Montero, S. *J. Chem. Phys.* **1984**, *80*, 4610−4619.
(56) Gough, K. M. *J. Chem. Phys.* **1989**, *91*, 2424−2432.
(57) Solchan, V. P.; Tildesley, D. J. *Faraday Discuss.* **1996**, *104*, 193−208.
(58) Schofield, D. A.; Goates, S. R.; Bain, C. D., unpublished results.
(59) Bell, G. R.; Manning-Benson, S.; Bain, C. D. *J. Phys. Chem. B* **1998**, *102*, 218−222.
(60) To calculate these angles, we used the procedure described in ref 9 and a value of $\beta_{aac}/\beta_{ccc} = 3.4$. Reducing the value of β_{aac}/β_{ccc} to 2 changes these angles by less than 1°.